JOURNAL OF MATERIALS SCIENCE 27 (1992) 4957–4961

Transmission electron microscopy analysis of a TiN_x substoichiometric CVD coating

J. L. DEREP, E. BEAUPREZ
E.T.C.A. Centre de Recherches et d'Etudes d'Arcueil, Departement "Physique des Surfaces", 16 Bis, Avenue Prieur de la Côte d'Or, 94114 Arcueil Cédex, France

The $TiN_x \square_{1-x}$ substoichiometric chemical vapour deposited titanium nitride coatings have been studied in an early work by means of high-resolution X-ray emission spectroscopy. It was found that a strong vacancy-induced peak was present in the Ti *K* emission band. Its intensity can be correlated to the $1-x$ vacancy concentration deduced from nuclear reaction spectroscopy and X-ray diffraction. This relationship is linear if $0 \leqslant 1 - x \leqslant 0.3$. If $1 - x$ is higher than 0.3, an anomalous behaviour occurs which is expected to be due to microstructure change. For this purpose, transmission electronic studies of a $TiN_{0.57} \square_{0.43}$ layer have been developed. The most striking result of this work is the existence of many stacking faults. These defects are extrinsic ones and the stacking fault energy is about 3.5 mJ m^{-2}. Their density seems to depend on their distance from the substrate–coating interface. Further investigations are needed to confirm this assumption.

1. Introduction

The transition metal carbides and nitrides belong to a class of compounds which combine metallic conduction with very high melting temperatures and extreme hardness normally associated with covalent bonding. They are used extensively as ultra-hard coatings for wear-resistant mechanical parts [1]. Titanium nitride films are at present those most studied and used in this class of hard coatings. The most successful application area of TiN is that of coatings on to various high-speed tools. Coatings with thicknesses of about 2–10 μm drastically increase the tool life [2, 3]. The use of TiN films as diffusion barriers in contact structures to silicon integrated circuits [4, 5] and solar cells [6] has also been investigated recently. TiN has also been studied as selective transparent films and for high-temperature photothermal conversion [7].

The transition metal carbides and nitrides mostly have the rock salt structure with non-metal atoms occupying the interstitial octahedral sites within the transition metal face centred cubic sublattice. They also exist as substoichiometric compounds over a large composition range with disordered vacancies at the non-metal sites (e.g. $0.41 \leqslant x \leqslant 1$ for TiN_x, where $x = N/Ti$). As a consequence, their physical properties (e.g. electrical conductivity or hardness [8]) which are controlled by the electronic structure, vary largely with composition. Therefore, to obtain a better understanding of the correlation between these physical properties and the N/Ti ratio, we have studied the electronic structure of substoichiometric TiN_x chemical vapour deposited (CVD) coatings by means of high-resolution X-ray emission spectroscopy (XES). A strong vacancy-induced peak occurs in the Ti *K* emission band [9–11]. Vacancy concentrations in these coatings have been deduced from nuclear reaction spectroscopy (NRS) and X-ray diffraction (XRD). The results emphasize a linear relationship between the vacancy peak intensity and the vacancy concentration for $0 \leqslant 1 - x \leqslant 0.3$. For higher apparent vacancy concentrations (NRS results), the peak intensity falls off [12]. Moreover, a very good agreement is obtained between the compositions given by NRS and XRD when $1 - x \leqslant 0.3$. Yet, the NRS vacancy concentration is systematically higher than the XRD one for $1 - x > 0.3$. This fact can be explained by either vacancy ordering or high fault density. Thus TEM microstructure has been performed on these special layers. The more interesting coating for which the greatest vacancy concentration difference was observed held our attention ($1 - x$ values are, respectively, 0.28 and 0.43 for XRD and NRS analysis).

Very few papers about TEM investigations on TiN_x CVD coatings can be found. TiN_x physical vapour deposited (PVD) coating microstructures are mainly studied and an exact chemical composition of these samples is not known [13–18]. Our work possibly constitutes the first attempt to establish a correlation between electronic structure, chemical composition and microstructure.

2. Experimental procedure

The titanium nitride coatings were obtained by CVD technique on a molybdenum substrate which was 0.3 mm thick. The layer thickness of $TiN_{0.57}$ was about 5 μm. TEM study of the titanium nitride ($TiN_{0.57}$) microstructure required thin foils which were obtained as follows. 3 mm diameter discs are cut from the $TiN_{0.57}$ coating (disc area was parallel to the

0022–2461

layer area). Then the opposite sides of the layer were mechanically polished until a 70 μm thickness (the sample then constituted the $TiN_{0.57}$ (5 μm) and the molybdenum substrate which was 60–65 μm thick). The molybdenum side was ion milled while the $TiN_{0.57}$ coating was protected by a varnish layer (see [11] for ion-milling conditions), this step was stopped when the $TiN_{0.57}$ coating appeared (the thin foil colour changes). Both sides were then ion milled (the varnish was removed prior to this step). A hole was then obtained with very thin sides (about 100 nm).

3. Results

The thin foils were observed parallel to the coating interface. The area which was studied by TEM was about $e/2$ deep where e is the $TiN_{0.57}$ thickness.

The microstructure of the coatings was constituted by equiaxed grains. Their size varied between 100 nm and 20 μm. They contained some defects such as dislocations and stacking faults, the latter being the most frequently encountered in the grains. Their arrangement was quite different from one grain to another. The stacking faults can be found as: alignments of defects in the same plane (Fig. 1); pile-ups (Fig. 2); tangles of stacking faults with different habit planes (Fig. 3); stair rods (Fig. 4); or isolated stacking faults (Figs 1, 2 and 4). Their density was not homogeneous. Some defects, like dark lines or dots (Fig. 4), were observed in all thin foils. They were situated on the top and bottom of the thin foils and were artefacts resulting from ion milling.

In summary, the main defects in the $TiN_{0.57}$ thin foils were stacking faults. Their density varied greatly in the areas investigated.

A detailed analysis of these defects was performed in order to determine their crystallographic and energetic parameters, such as: partial dislocations with their $\vec{b}_p$ Bürgers vectors and $\vec{u}$ direction line; the habit plane of the defect; the $\vec{R}_f$ displacement vector; their nature (intrinsic or extrinsic); and the γ stacking fault energy.

Two kinds of stacking fault were studied: an isolated fault F_1 (Fig. 5) and a second defect F_2 (Fig. 1)

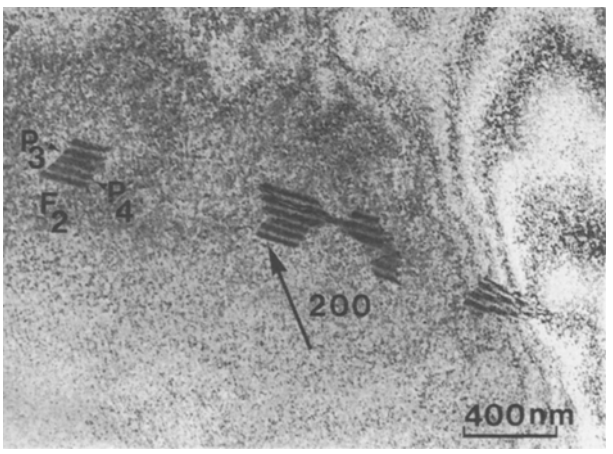

Figure 1 Stacking faults encountered in $TiN_{0.57}$ coating, the fault plane of each defect is in the same habit plane (i.e. {1 1 1}).

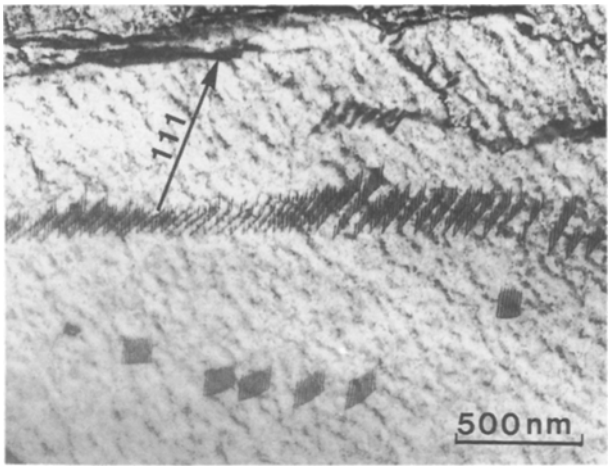

Figure 2 Pile-up of stacking faults, their fault planes are parallel (unlike Fig. 1).

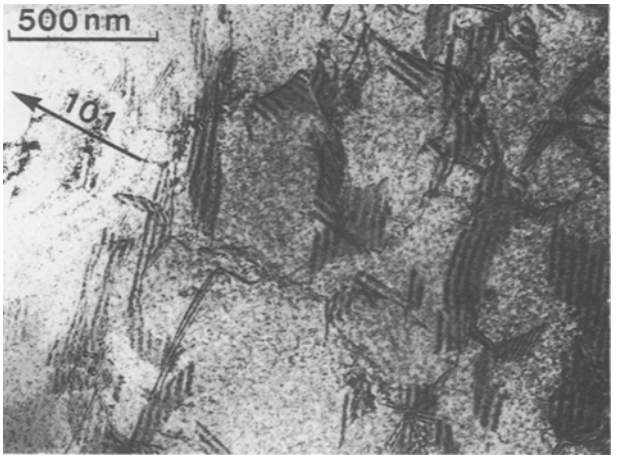

Figure 3 Tangles of stacking faults with different habit planes.

which is part of an alignment. The fringe symmetry observed in dark- and bright-field images give us the nature (extrinsic or intrinsic) of the defect [19]. So, for example, from the fringe system obtained for the F_1 defect using the diffracted beam $\vec{g} = (2\,0\,0)$ (Fig. 6), we can deduce the extrinsic nature of the F_1 stacking fault.

The partial dislocations of the F_1 defect were also studied. Their $\vec{u}$ line vector was obtained using the stereographic projection of the dislocation image normals (Fig. 7). The $\vec{u}$ vector is parallel to the $[\bar{1}\,0\,1]$ direction for both dislocations P_1 and P_2. If the $\vec{g}\cdot\vec{b}_p = 0$ and $\vec{g}\cdot(\vec{b}_p \wedge \vec{u}) = 0$ extinction criteria are applied to determine the Burgers vectors of the P_1, P_2 and P_3, P_4 partial dislocations (Fig. 8 and Figs 1 and 9, respectively), we obtain $\vec{b}_{p_1} = 1/6\,[\bar{2}\,1\,1]$, $\vec{b}_{p_2} = 1/6\,[1\,\bar{1}\,2]$, $\vec{b}_{p_3} = 1/6\,[\bar{2}\,1\,1]$ and $\vec{b}_{p_4} = 1/6\,[1\,0\,1]$. P_1, P_2 and P_3 are Shockley dislocations while P_4 is a Lomer–Cottrell or "stair rod" dislocation. P_4 is the combination result of the two Shockleys which are partial dislocations of F_2 and F'_2 stacking faults on two different habit planes (Fig. 9).

In summary, the stacking fault observed in this TiN layer is the result of the dissociation of one perfect dislocation to give two Shockleys which are characterized by $\vec{b}_p = 1/6\langle 1\,1\,2\rangle\,\vec{u} = \langle 1\,0\,1\rangle$.

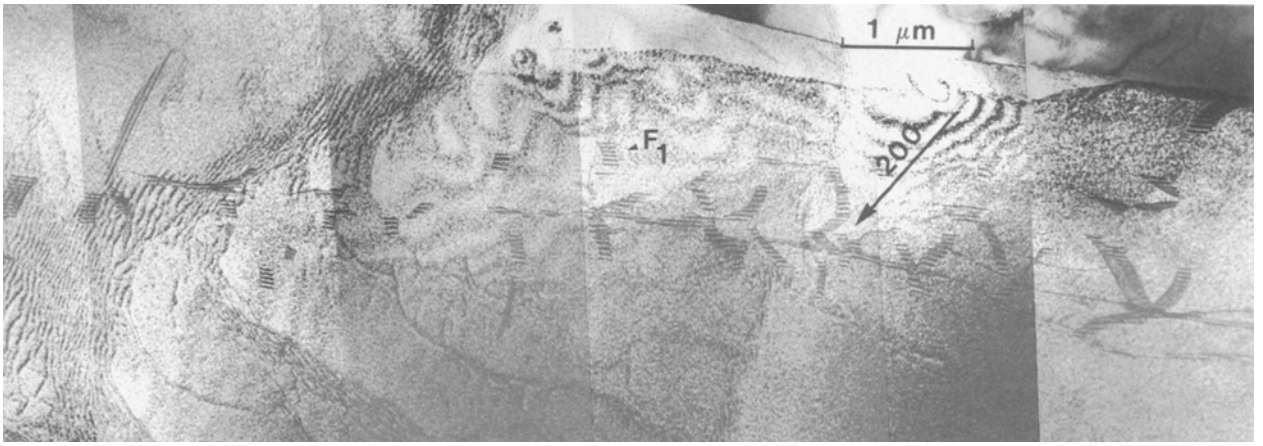

Figure 4 Interactions between different habit plane stacking faults to form stair-rods.

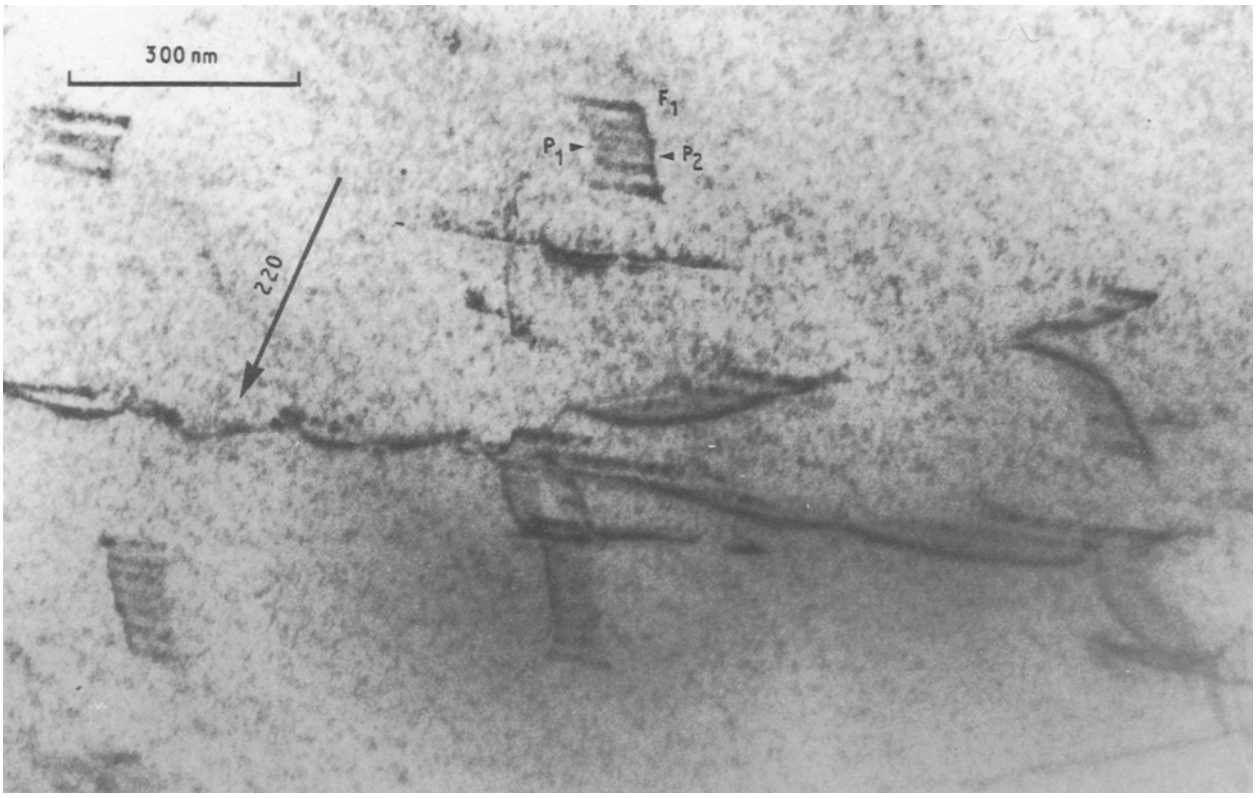

Figure 5 Analysis of F_1 isolated stacking fault: F_1 is limited by two Shockley dislocations, P_1 (out of contrast) and P_2 (in contrast).

The habit plane of F_1 and F_2 stacking faults is obtained from the result of the $\vec{b}_p \wedge \vec{u}$ relation. So F_1 and F_2 are on the (1 1 1) habit plane while F_2' is on the $(1\,\bar{1}\,1)$ Plane.

The phase difference produced by the F_1 and F_2 stacking faults is given by $\alpha = 2\pi\vec{g}\cdot\vec{R}_f$ with $\vec{g}$, the diffracted beam and $\vec{R}_f$, the displacement vector. If $\alpha = 0(2\pi)$ or $\alpha = \pm 2\pi/3(2\pi)$, the fault is, respectively, invisible or in contrast. As shown in Fig. 9a–c, for $(\bar{2}\,0\,2)$, $(\bar{1}\,\bar{1}\,1)$ and $(1\,1\,\bar{1})$ beams, respectively, α is equal to 0 (2π), $-2\pi/3(2\pi)$ and $2\pi/3(2\pi)$. Then the $\vec{R}_f$ displacement vector is equal to either $1/6\langle 1\,2\,1\rangle$ or $1/3\langle 1\,1\,1\rangle$ owing to the extrinsic nature of the stacking faults. To determine the exact $\vec{R}_f$ vector, a comparison between experimental and computed images is required.

The energy which is needed to create a stacking fault (in the isotropic elasticity approximation) is given by the following relationship [20]

$$\gamma = \left(\frac{\mu}{4\pi}\right)\left(\frac{\vec{b}_1\cdot\vec{b}_2}{d_0}\right)\left(\frac{(2-\nu)}{(1-\nu)}\right) \quad (1)$$

where d_0 is given by

$$d = d_0\{\cos(\theta) - [\nu/(2-\nu)]\cos(2\varphi + \beta_2 - \beta_1)\} \quad (2)$$

with $\theta = (\vec{b}_1, \vec{b}_2)$, $\beta_1 = (\vec{b}_1 + \vec{b}_2, \vec{b}_1)$, $\beta_2 = (\vec{b}_1 + \vec{b}_2, \vec{b}_2)$,

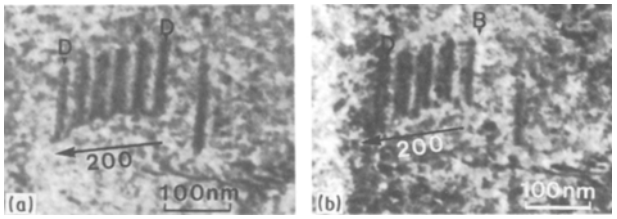

Figure 6 The nature of the F_1 stacking fault, $\vec{g}$ (A class of Bragg reflections) points towards the dark fringe; F_1 is an extrinsic stacking fault. (a) Two-beam bright-field image $\vec{g} = (2\,0\,0)$, the top and bottom fringes are dark (D). (b) Two-beam dark-field image $\vec{g} = (2\,0\,0)$, the top fringe is dark (D) and the bottom is bright (B).

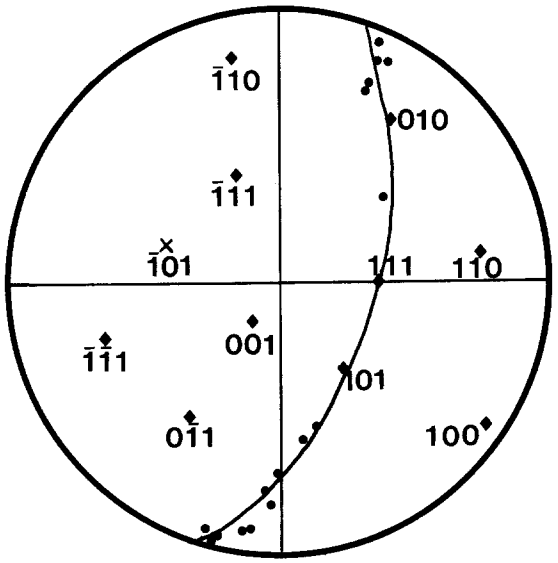

Figure 7 Direction line ($\vec{u}$) determination of P_1 and P_2 partial dislocations; normals to the dislocation line projection determine a plane, the pole of this one corresponds to the $\vec{u}$ direction line of the dislocations: $\vec{u} = [\bar{1}\,0\,1]$.

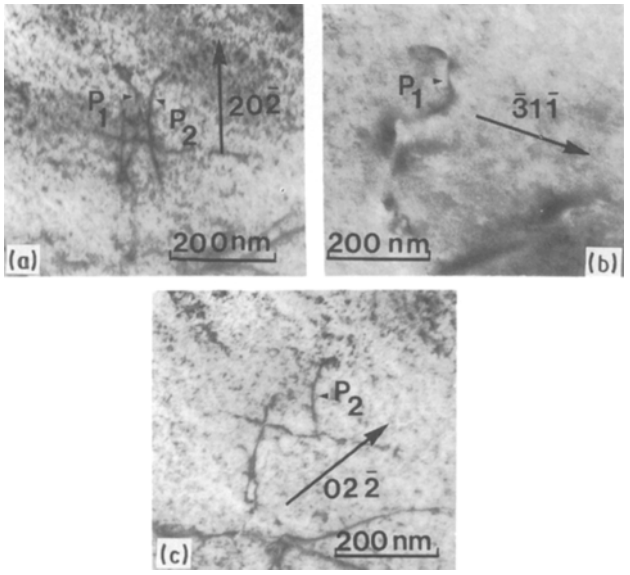

Figure 8 P_1 and P_2 bright-field images (two-beams condition with the fault is out of contrast), determination of the Burgers vectors: $\vec{b}_{p_1} = 1/6\,[\bar{2}\,1\,1]$ and $\vec{b}_{p_2} = 1/6\,[\bar{1}\,\bar{1}\,2]$. (a) P_1 and P_2 dislocations are in contrast, (b) P_1 is in contrast and P_2 is invisible, (c) P_1 is out of contrast and P_2 is visible.

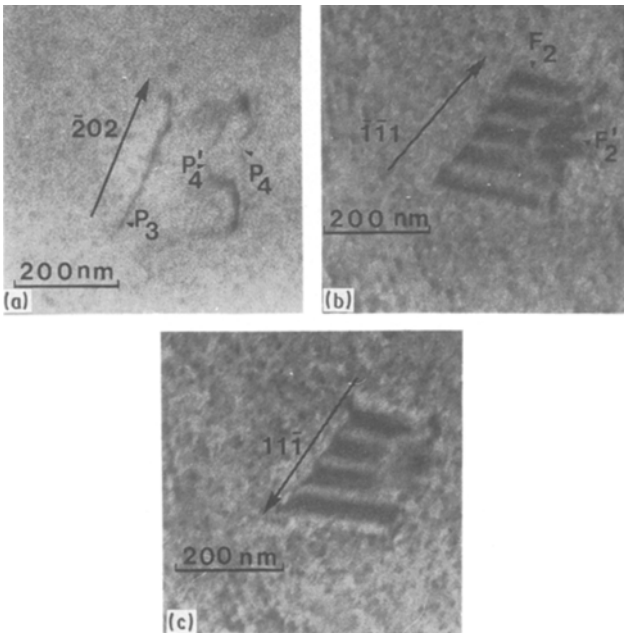

Figure 9 Two-beam bright-field images of the F_2 stacking fault. F_2 is not isolated; there is a stair-rod dislocation, P_4, which is the result of the reaction between the two stacking faults, F_2 and F_2'. (a) The fault F_2 is out of contrast, three partial dislocations are observed, P_3, P_4 and P_4'. (b) The fault F_2 is visible and reveals the existence of a second fault, F_2', which forms a stair-rod with F_2. (c) Same image as in (b) made with the opposite $\vec{g}$ to show the extrinsic nature of F_2.

$\varphi = (\vec{u}, \vec{b}_1 + \vec{b}_2)$, ν the TiN Poisson coefficient, μ its shear modulus and $\vec{b}_1, \vec{b}_2, \vec{u}$ are the Burgers and line vectors of the partial dislocations. So, for P_1 and P_2

$$\begin{aligned} \|\vec{b}_1\| &= \|\vec{b}_2\| = a/6^{1/2}, \\ \beta_1 &= \beta_2 = \pi/6 \end{aligned} \tag{3}$$

and for P_3, P_4

$$\begin{aligned} \|\vec{b}_3\| &= a/6^{1/2}, \quad \|\vec{b}_4\| = a/18^{1/2}, \\ \beta_3 &= 33.6^\circ, \quad \beta_4 = 73.2^\circ \end{aligned} \tag{4}$$

where $a = 0.4225$ nm [11] is a reticular parameter of TiN.

For F_1 and F_2, the d length between P_1 and P_2, P_3 and P_4 is, respectively, equal to 136 and 205 nm. Then the γ stacking fault energy is equal to 3.7 and 2.2 mJ m^{-2} ($\mu = 240$ GPa, $\nu = 0.20$ [21]). The mean value for the calculated stacking fault energy is about 3 mJ m^{-2}. This value is often encountered in the face centred materials containing substitutional elements [22] or vacancies [23]. The relationship between γ and d is made on the assumption that TiN is an isotropic material. If this is not true, the stacking fault energy may be larger than the calculated value. To confirm this, the matrix of C_{ij} $TiN_{0.57}$ elastic coefficients is needed. But at present, it is unknown.

To summarize the different results, the $TiN_{0.57}$ stacking faults characteristics are:

nature of defect	extrinsic
partial dislocations	$\vec{b}_p = 1/6\langle 1\,1\,2\rangle, \vec{u} = \langle 1\,0\,1\rangle$
habit plane	$\{1\,1\,1\}$
displacement	$1/3\langle 1\,1\,1\rangle$ or $1/6\langle 1\,1\,2\rangle$
stacking fault energy	≈ 3 mJ m^{-2}

4. Conclusions

The most important characteristic of the sub-stoichiometric TiN coating is the existence of many extrinsic stacking faults. The energy of these defects varies with the vacancy or impurity concentration in TiN. The defect density seems to change strongly with the distance between the mean plane observation and the substrate interface. As the N/Ti ratio is lower than 1 (stoichiometric value), the $TiN_{0.57}$ coatings contain an excess of titanium atoms. Neither titanium grains nor any other phase (such as Ti_2N, for example) were observed by TEM or by X-ray diffraction [11]. So it seems likely that extrinsic stacking faults were made by the coalescence of titanium atoms in the (1 1 1) planes of a TiN_y where y has a value near the stoichiometric value [24]. This assumption can explain the too high crystal parameter measured for this nitrogen concentration ($a = 0.4225$ nm compared with the expected value $a = 0.4219$ nm [11, 12]). For N/Ti lower than 0.7, the a crystal parameter was found to be higher than the calculated one [11, 12]. This computed value was obtained from NRS spectroscopy using Nagakura *et al.*'s relationship between the lattice parameter and chemical composition [25]. A limiting N/M (M = Ti, V, . . .) ratio seems to exist for which the stacking fault energy (for the face centred structure) of the MN_x nitrides is low enough to give a high stacking fault density [26]. It will be very convenient to use contrast simulation correlated with high-resolution electron microscopy to determine the exact crystallographic structure of these faults. Thin foils were observed in a plane parallel to the substrate coating interface. Therefore, the distribution heterogeneity of the stacking faults in the coating thickness must be confirmed by transverse observations of the coatings.

References

1. J. E. SUNDGREN and H. T. G. HENTZELL, *J. Vac. Sci. Technol.* **A4** (1986) 2259.
2. B. COLL and P. COLLIGNON, *Traitement thermique* **184** (1984) 19.
3. J. E. SUNDGREN, *Thin Solid Films* **128** (1985) 21.
4. W. WITTMER and H. MELCHIOR, *ibid.* **93** (1982) 397.
5. T. BRAT, N. PARIKH, N. S. TSAI, A. K. SINHA, J. POOLE and C. WICKERSHAM Jr, *J. Vac. Sci. Technol.* **B5** (1987) 1741.
6. M.-A. NICOLET, *Thin Solid Films* **52** (1978) 415.
7. B. KARLSSON, R. P. SHIMSHOCK, B. O. SERAPHIN and J. C. HAYGARTH, *Phys. Scripta* **25** (1982) 775.
8. J. E. SUNDGREN, B. O. JOHANSSON, A. ROCKETT, S. A. BARNETT and J. E. GREENE, in "A. I. P. Conference Proceedings (USA) no. 149" (1986) p. 95.
9. E. BEAUPREZ, C. F. HAGUE, J.-M. MARIOT, F. TEYSSANDIER, J. REDINGER, P. MARKSTEINER and P. WEINBERGER, *Phys. Rev.* **B34** (1986) 886.
10. E. BEAUPREZ, C. F. HAGUE and J.-M. MARIOT, in "Proceedings of International Symposium on Trends and New Applications in Thin Films", Strasbourg, Vol. 2, 16–20 March 1987, p. 397; Supplément à la revue "Le Vide, les Couches Minces" no. 235.
11. E. BEAUPREZ, Thesis, University Pierre et Marie Curie, Paris 6 (1989).
12. E. BEAUPREZ, S. HAREL, J.-L. DEREP, N. MONCOFFRE, J. TOUSSET, J.-M. MARIOT and C. F. HAGUE, in "Proceedings of the 1st European Ceramic Society Conference", Maastricht, Vol. 2, 18–23 June 1989, edited by G. de With, R. A. Terpstra and R. Metselaar (Elsevier Applied Science, London) p. 125.
13. M. K. HIBBS, B. O. JOHANSSON, J. E. SUNDGREN and U. HELMERSON, *Thin Solid Films* **122** (1984) 115.
14. L. J. WAN and Z. K. HEI, *Scripta Metall.* **23** (1989) 213.
15. B. E. JACOBSON, R. NIMMAGADDA and R. F. BUNSHAH, *Thin Solid Films* **63** (1979) 333.
16. M. K. HIBBS, J. E. SUNDGREN, B. O. JOHANSSON and B. E. JACOBSON, *Acta Metall.* **33** (1985) 797.
17. K. Y. AHN, M. WITTNER and C. Y. TING, *Thin Solid Films* **107** (1985) 45.
18. F. ABAUDET and P. EVENO, *Rev. Phys. Appl.* **25** (1990) 1113.
19. S. AMELINCKX, *Solid State Phys. Suppl.* **6** (1964) 445.
20. F. R. N. NABARRO, *Dislocat. Crystals, Dislocat. Solids* **2** (1982) 74.
21. Metals and Ceramics Information Center, Report HB-07, 1–2 (1979), Battelle Columbus Laboratories, OH, USA.
22. G. THOMAS, "Transmission Electron Microscopy of Metals" (Wiley, New York, London, 1962) p. 203.
23. J. L. MARTIN, P. LACOUR-GAYET and P. COSTA, in "Electron Microscopy and Structure of Materials", edited by G. Thomas (University of California Press, Berkeley, Los Angeles, London, 1972) p. 1131.
24. V. MOISY-MAURICE and C. H. de NOVION, *J. Phys. France* **49** (1988) 1737.
25. S. NAGAKURA, T. KUSUNOKI, F. KAKIMOTO and Y. HIROTSU, *J. Appl. Crystallogr.* **8** (1975) 65.
26. M. H. LEWIS, J. BILLINGHAM and P. S. BELL, in "Electron Microscopy and Structure of Materials", edited by G. Thomas (University of California Press, Berkeley, Los Angeles, London, 1972) p. 1084.

Received 17 June
and accepted 16 December 1991